

# Magnetic Field Scaling of the Conductance of Epitaxial Cuprate-Manganite Bilayers.

P. A. Kraus<sup>\*†</sup>, A. Bhattacharya<sup>†</sup>, and A. M. Goldman  
*School of Physics and Astronomy, University of Minnesota,*  
*116 Church St. SE, Minneapolis,*  
*MN 55455, USA*  
 (July 20, 2001.)

Conductance-voltage characteristics of epitaxial interfaces between oxide ferromagnets and oxide superconductors have been measured as a function of temperature and magnetic field. Their functional form is similar to that predicted by theories of transport across nearly transparent contacts between highly spin-polarized ferromagnets and *d*-wave superconductors. However, their magnetic field dependencies scale in striking and unusual ways, challenging our current understanding. Existing theories fail to account for apparent nonequilibrium effects that are natural for spin injection in such geometries.

PACS numbers: 72.25.-b, 72.25.Rb, 74.80.Dm, 72.25.Mk

The half-metallicity of the alkaline earth doped lanthanum manganites leads to their charge carriers being spin-polarized [1]. This, together with the epitaxial compatibility of these oxide ferromagnets and oxide superconductors [2], has led to the use of such heterostructures for the study of spin injection [3] in the cuprates [4–6,8,9]. This has motivated a number of theoretical papers [10–15], most of which describe interfaces of varying transparency exhibiting suppression of Andreev reflection, but except for Refs. [14] and [15] do not consider nonequilibrium effects. In this Letter we report on conductance-voltage characteristics,  $G(V)$ , of cuprate/manganite heterostructures, with no buffer layer between the cuprate and manganite. The geometry is arranged so that the current density is uniform across the area of contact between the superconductor and the ferromagnet. The zero-bias conductance peak (ZBCP) reported by other groups [17–19] is absent. Furthermore, as a function of temperature and magnetic field, striking and unusual scaling of the data at low bias is found. This observation puts a serious constraint on any theory, and conversely, a theory that explains all the features of the data might allow for the intriguing possibility of gap spectroscopy of superconductors using such structures. A complete description would have to account for nonequilibrium effects of spin injection on the underlying superconductor.

Epitaxial heterostructures consisting of *c*-axis oriented  $\text{DyBa}_2\text{Cu}_3\text{O}_{7-\delta}$  (DBCO, 50 nm thick) and  $\text{La}_{2/3}\text{Ba}_{1/3}\text{MnO}_3$  (LBMO, 40 nm thick) capped with Au (50 nm thick) were grown *in situ* on epitaxially polished  $\text{SrTiO}_3$  substrates using ozone-assisted molecular beam epitaxy in the block-by-block mode [20,21]. The

as-grown buried DBCO layer was not superconducting, necessitating an oxygen annealing step, which took a few days. The superconducting transition temperatures ( $T_c$ ) of the DBCO layers were all about 70 K, a consequence of their being underdoped. The interfaces were of high quality, with cross-sectional transmission electron microscopy demonstrating heteroepitaxy of the layers over semi-macroscopic distances, and *in situ* RHEED studies carried out during growth suggesting very abrupt transitions between layers.

The Au and LBMO were patterned into rectangles 10  $\mu\text{m}$  wide, with varying lengths, on a 10  $\mu\text{m}$  wide strip of the underlying DBCO film (Fig.1). Electrical leads were patterned for vertical four-terminal measurements of  $G(V)$  through each structure. The Au layer provided an equipotential surface, and forced the current to traverse the numerous interfaces in a vertical direction (parallel to the *c*-axis). During such measurements, no current flowed in the plane of the manganite layer. Additional leads permitted simultaneous four-terminal measurements of the superconducting layer.

Figure 2 shows plots of  $G(V)$ , at several temperatures of a structure, 10  $\mu\text{m} \times 20 \mu\text{m}$  in area. Not shown is the voltage-independent conductance observed above  $T_c$ . There are several features of these curves, which should be noted: below  $T_c$  a zero-bias conductance peak appears. As the temperature is reduced, this transforms into a plateau, and then into a "vee"-shaped dip, which deepens with decreasing temperature. The maxima in  $G(V)$  at  $\pm 40$  mV found at low temperatures are followed by a rapid fall off, while for a 10  $\mu\text{m} \times 10 \mu\text{m}$  structure, they occur at about  $\pm 80$  mV. These features cannot be associated with the superconducting gap amplitude as their value would be unphysically large for an underdoped film. In fact, the observed maxima actually mark the beginning of the demise of superconductivity due to current injection. At 2 K, the underlying DBCO strip is driven normal by an injection current through the ferromagnet of about 66 mA, while 86 mA is required if injection is in the plane. Control experiments in which the manganite was replaced by either Au or  $\text{LaNiO}_3$  films in similar geometries and with the same resistances show no nonlinear effects in  $G(V)$  at similar current densities. This supports the view that the effects are not a consequence of heating and are due to spin rather than charge injection [5,6]. Estimates of power dissipation under injection conditions suggest a temperature rise of at most

1 K, which is also not sufficient to account for the observations. The inset shows a monotonous increase in the zero-bias resistance of the trilayer on cooling below  $T_c$ , contrary to what one would expect for resistance at grain boundaries in the manganite [7].

The magnetic field dependences of  $G(V)$ , at temperatures from 2 K to 70 K are shown in Fig.3. The field is applied in the plane of the cuprate/manganite interface. The qualitative effect of increasing field is similar to that of increasing temperature. This is dramatically borne out by the inset. Similar results were reported in our earlier work on geometries in which the current density was not uniform [5]. There is a small asymmetry in the  $G(V)$  which grows with increasing magnetic field and decreasing temperature.  $[G(V+) - G(V-)]/G(V)$  is less than 5% at 12 T and 2 K.

Notable by its absence at low temperatures is the zero-bias conductance peak (ZBCP) that has been reported in other experiments [18,19]. This peak is usually attributed to sub-gap Andreev bound states, which occur for tunneling in the  $a$ - $b$  directions (maximally along (110) directions) into a cuprate superconductor, because of the change of sign in the  $d$ -wave order parameter on rotation by an angle of  $\pi/2$  in the  $a$ - $b$  plane [17]. The present epitaxial  $c$ -axis oriented films are relatively free of such  $a$ - $b$  facets at the cuprate/manganite interface. For spin polarized injection in this geometry, the effective gap is an angular average over all directions, and this suppresses the ZBCP. Also, for an interface with high transparency, one would expect the ZBCP to disappear.

A very striking and unusual feature of the data is shown in Fig. 4, where we have plotted  $G(V,H)/G(0,H)$  for different values of  $H$  at a fixed temperature. All curves in various magnetic fields collapse onto a single curve at a fixed temperature. This works at each temperature, but with a functional form that is different in detail. The difference may be due to an increase of the quasiparticle population in the superconductor with temperature, and/or a change in the spin polarization of carriers in the manganite [22]. This collapse at low bias has been observed in all devices measured, at all fields and temperatures where a minimum in  $G(V)$  is clearly seen. This implies that at low bias voltages,  $G(V,H,T)=h(H,T)g(V,T)$ . At a fixed temperature, the collapsed curve is essentially  $g(V,T)$ . The field dependent prefactor, normalized by its value at zero field, i.e.  $h(H,T)/h(0,T)$ , is shown in Fig. 5. At the lowest temperatures of 2 K and 10 K, it is fit very well by a straight line. In fact, the 2 K and 10 K data lie nearly on top of each other. At higher temperatures, though still very close to linear,  $h(H,T)$  deviates slightly from the straight line fit at 2K. This kind of collapse is also suggested by the data of Sawa *et al.* at high bias voltages [18], although at low bias it is obscured by the ZBCP. In our data we also observe that plots  $G(0,T)/G(0,T = 2K)$  at all applied magnetic fields, seem to have very similar

temperature dependences (see Fig. 5, inset).

We note that the zero-bias conductance  $G(0)$  increases by about a factor of two when temperature is increased from 2 K to 10 K, keeping the magnetic field fixed. Correspondingly, on increasing the magnetic field up to 12 T and keeping the temperature fixed, the zero-bias conductance again increases by a factor of about two. Considering that  $\mu_B \Delta H \approx k_B \Delta T$  for  $\Delta H = 12$  T and  $\Delta T = 8$  K, one might conclude that the measurements are probing the density of states near the nodes [11] of a  $d$ -wave like gap, with the increase in conductance corresponding to an increase in the number of accessible states. If there is suppression of Andreev reflection at the ferromagnet/superconductor interface, then  $G(V)$  probes the density of states of the superconductor [11]. Motivated by this, and presuming a small barrier at the cuprate/manganite interface, we have calculated temperature and magnetic field dependence for the conductance-voltage curves at the interface between a half-metallic ferromagnet and a  $d$ -wave superconductor using a simple tunneling expression [16]

$$I(V) \sim \int_{-\infty}^{\infty} \nu_{fm} \nu_s(E + \mu H) \{f(E + eV) - f(E)\} dE. \quad (1)$$

Here the density of states for quasiparticles in a  $d$ -wave superconductor  $\nu_s(E) \sim \nu_n(E/\Delta_o)$ ,  $\Delta_o$  is the gap amplitude,  $f$  is the Fermi function, and  $\nu_n$  is the density of states at the Fermi energy of the superconductor in the normal state. The density of states in the ferromagnet  $\nu_{fm}(E)$  is assumed constant. Applying a magnetic field enhances the density of states for quasiparticles of one spin species at the expense of the other, enhancing conductance for carriers of the predominant spin across the interface. We plot  $G(V) = dI/dV$  as a function of applied magnetic field and temperature at low applied bias (Fig. 6).  $G(V)$  increases linearly as a function of  $H$  at all bias voltages. This suggests that the spin polarization of carriers plays a role in the enhancement of conductance in the experiment. The calculated increase in  $G(0)$  is the same when  $T$  increases from 2 K to 10 K with  $H = 0$ , and when  $H$  increases from 0 T to 12 T at  $T = 2$  K, which is by a factor of about five. This increase is greater, though of the same order of magnitude as that seen in the experiment. However, the scaling of the experimental data indicates that the application of magnetic field has a *multiplicative* effect on the conductance, with the increase being greater at higher bias voltages. This leads us to believe that the explanation of this phenomenon involves physics different from that of our simple argument.

In choosing to ensure that currents flowed vertically through the structure, we added a gold overlayer. This compromised our ability to make true four terminal measurements of the cuprate/manganite interface, as the re-

sultant gold/manganite series resistance cannot be subtracted in any systematic fashion. The  $10\ \mu\text{m} \times 20\ \mu\text{m}$  gold/manganite/cuprate trilayer structure has a zero-bias resistance of about  $1.46\ \Omega$  at 10 K. From other measurements, the gold/manganite interface resistance is known to be ohmic. Assuming that the linear field dependence of  $G(V,H)$  occurs due to the cuprate/manganite interface, the field independent ohmic part of the trilayer resistance can be extracted from the data near zero-bias, and is about  $0.06\ \Omega$  at 10 K. The gold/manganite interface resistance is presumably a fraction of this value. At higher injection currents where the trilayer resistance ( $V/I$ ) is about  $0.5\ \Omega$ , the contact resistance of the gold/manganite interface is a greater fraction of the total resistance, and the actual voltage across the cuprate/manganite interface near the peaks in  $G(V)$  may be significantly smaller than the measured voltage.

Given the values of specific interface resistances (gold/manganite + manganite/cuprate), which were of order  $10^{-6}\ \Omega - \text{cm}^2$ , the interfaces are highly transparent, but certainly not ballistic. Thus the striking voltage dependence of  $G(V)$  at low bias, although reminiscent of suppressed Andreev reflection [10–12], cannot be explained by that alone. Furthermore, injection of spin-polarized quasiparticles into a superconductor creates a steady-state spin imbalance analogous to the spin imbalance created by the application of a magnetic field due to Zeeman splitting of the spin energies [13]. This leads to a suppression of the superconducting order parameter near the manganite/cuprate interface. Also, the voltage drop due to injection of these spin-polarized quasiparticles would then occur over a characteristic relaxation length in the superconductor, and not abruptly at the interface (as in the case of tunneling). If this relaxation length is sufficiently large in the cuprate, the measured voltage would not be the spectroscopic voltage of the interface. Thus, the absence of any signatures of the coherence peak in  $G(V)$  may be because the superconductor near the boundary is driven normal before the voltage across the manganite/cuprate interface reaches a value corresponding to the gap amplitude. This situation is not part of any of the theories as the pair potential is assumed to be constant as a function of distance from the interface, and independent of current.

This work was supported by the Office of Naval Research under Grant N/N00014-98-1-0098. The authors would like to thank J.P. Locquet, V. Vas'ko, V. Larkin, A.I. Larkin and L.I. Glazman for useful discussions.

\*Present address: Applied Materials Inc., Santa Clara, CA.

†Authors contributed equally to this work.

- [1] For a review see: A. Ramirez, *J. Phys.: Condens. Matter* **9**, 8171 (1997).
- [2] K. Chahara *et al.*, *Appl. Phys. Lett.* **63**, 1990 (1993).
- [3] Mark Johnson and R. H. Silsbee, *Phys. Rev. B* **37**, 5326 (1988); The first spin injection study of a cuprate involved the use of Permalloy. See: Nir Hass *et al.*, *Physica C* **235-240**, 1905 (1994).
- [4] V. A. Vas'ko *et al.*, *Phys. Rev. Lett.* **78**, 1134 (1997).
- [5] V. A. Vas'ko *et al.*, *Appl. Phys. Lett.* **73**, 844 (1998).
- [6] Z. W. Dong *et al.*, *Appl. Phys. Lett.* **71**, 1718 (1997).
- [7] N.K. Todd *et al.*, *J. App. Phys.* **85**, 7263 (1999).
- [8] R. M. Stroud *et al.*, *J. Appl. Phys.* **83**, 7189 (1998).
- [9] N-C. Yeh *et al.*, *Phys. Rev. B* **60**, 10522 (1999).
- [10] I. Zutic and O. T. Valls, *Phys. Rev. B* **60**, 6320 (1999); I. Zutic and O. T. Valls, *Phys. Rev. B* **61**, 1555 (2000).
- [11] S. Kashiwaya *et al.*, *Phys. Rev. B* **60**, 3572 (1999); Y. Tanaka and S. Kashiwaya, *Phys. Rev. Lett.* **74**, 3451 (1995); J. H. Xu, J. H. Miller and C. S. Ting, *Phys. Rev. B* **53**, 3604 (1996).
- [12] Jian-Xin Zhu, B. Friedman, and C. S. Ting, *Phys. Rev. B* **59**, 9558 (1999).
- [13] S. Takahashi, H. Imamura, and S. Maekawa, *Phys. Rev. Lett.* **82**, 3911 (1999).
- [14] A.A. Golubov, *Physica C* **326-327**, 46 (1999).
- [15] F.J. Jedema *et al.*, *Phys. Rev. B* **60**, 16549 (1999).
- [16] R. Meservey and P.M. Tedrow, *Phys. Rep.* **238**, 173-243 (1994).
- [17] M. Covington *et al.*, *Phys. Rev. Lett.* **79**, 277 (1997).
- [18] A. Sawa *et al.*, *cond-mat/9908431*.
- [19] Z. Y. Chen *et al.*, *cond-mat/0007353*.
- [20] J.-P. Locquet *et al.*, *Appl. Phys. Lett.* **64**, 372 (1994).
- [21] V. A. Vas'ko *et al.*, *Appl. Phys. Lett.* **68**, 2571 (1996).
- [22] J. Y. T. Wei, N.-C. Yeh, and R. P. Vasquez, *Phys. Rev. Lett.* **79**, 5150 (1997); J-H. Park *et al.*, *J. Appl. Phys.* **79**, 4558 (1996); Moon-Ho Jo *et al.*, *Phys. Rev. B* **61**, 1495 (2000).

FIG. 1. Device geometry for vertical spin injection. I2/V2 and I3/V3 are used to measure the LBMO/DBCO interface, while I1/V1 and I3/V3 are used to characterize the DBCO.

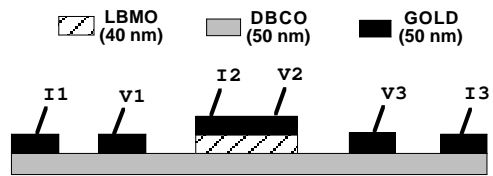
FIG. 2.  $G(V)$  for a Au/LBMO/DBCO heterostructure, of area  $10\ \mu\text{m} \times 20\ \mu\text{m}$ . The curves show a conductance peak at the highest temperature. At low temperature, the  $G(V)$  data are rounded at low bias, tending to two arms of a 'vee' shape at higher bias, before falling abruptly as the underlying superconductor is quenched. The inset shows the zero bias conductance of the trilayer as a function of temperature.

FIG. 3.  $G(V)$  in magnetic fields applied parallel to the plane for a  $10\ \mu\text{m} \times 20\ \mu\text{m}$  device at 10 K. The inset shows data at 65 K.

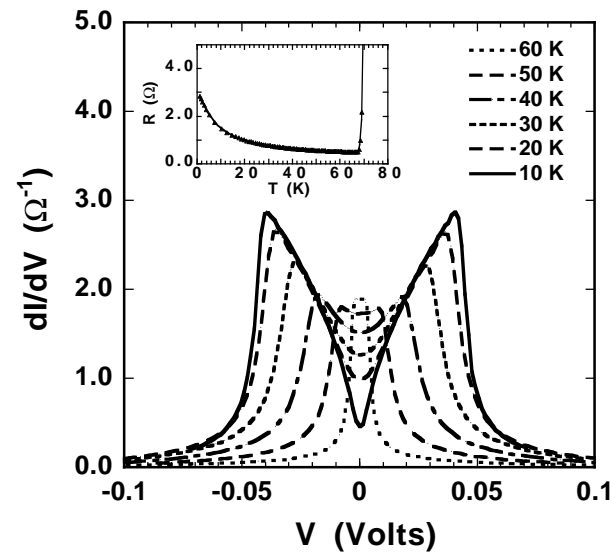
FIG. 4. Conductance data at 10 K normalized by the zero bias conductance at each magnetic field, plotted vs. voltage for the  $10\ \mu\text{m} \times 20\ \mu\text{m}$  device. The data collapse onto a single curve at low bias for all applied magnetic fields up to 12 T.

FIG. 5.  $G(0)$  for the  $10\ \mu\text{m} \times 20\ \mu\text{m}$  device plotted vs. magnetic field  $H$  applied parallel to the plane, at different temperatures. The data are normalized to the conductance at  $H = 0$ . A straight line is fit to the data at  $2\text{K}$  as a guide to the eye. The inset shows  $G(0)$  plotted as a function of temperature at different values of magnetic field. The data at each magnetic field are normalized to the value of the conductance at  $T = 2\text{K}$ .

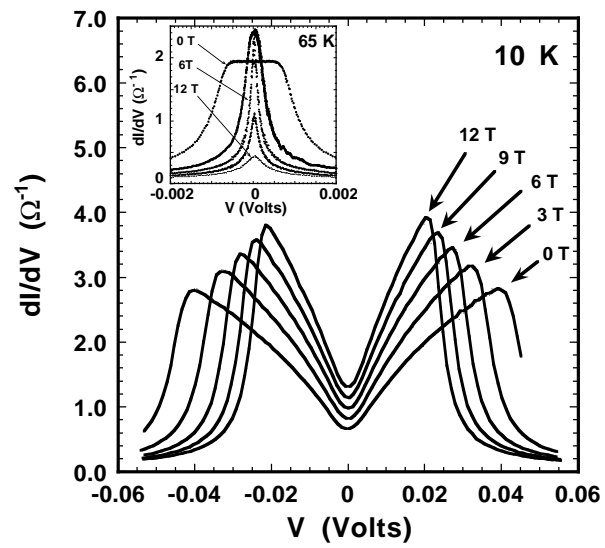
FIG. 6.  $G(V)$  calculated using density of states form from Eq. 1. for spin injection from a half-metallic ferromagnet. The change in conductance on applying magnetic field from  $0\text{ T}$  to  $12\text{ T}$  at  $2\text{ K}$  is compared to the change caused by increasing the temperature from  $2\text{ K}$  to  $10\text{ K}$  at  $0\text{ T}$ (inset).



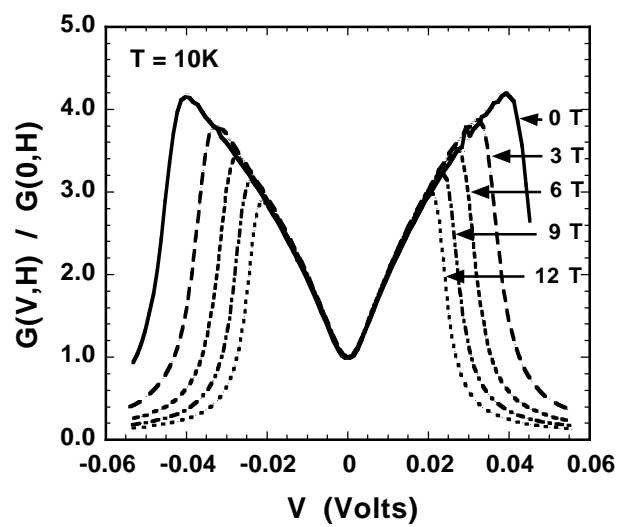
P.A. Kraus et al.  
FIG. 1.



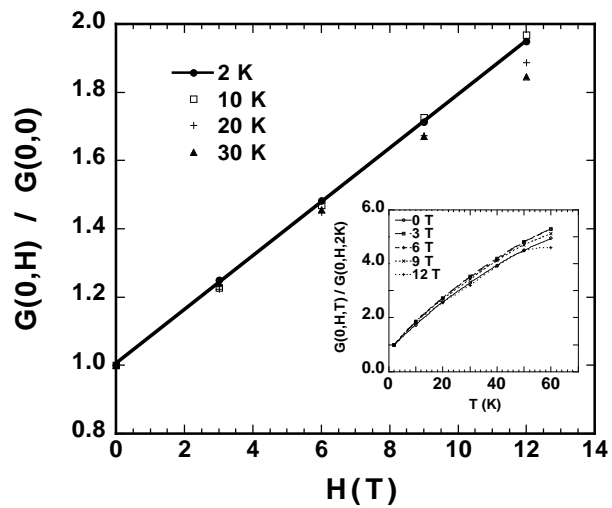
P.A. Kraus et al.  
FIG. 2.



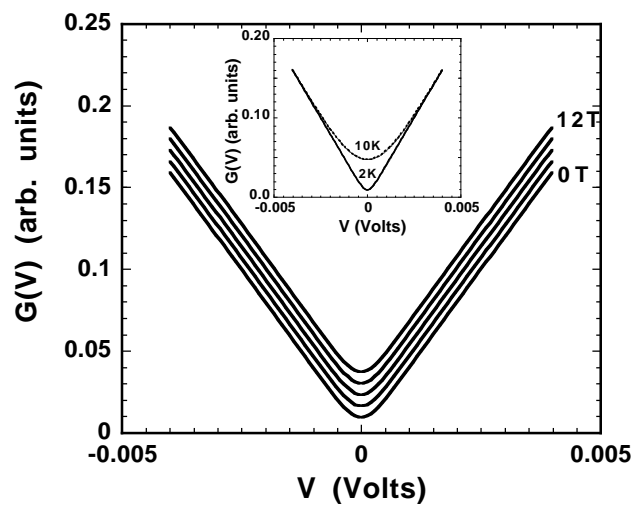
P.A. Kraus et al.  
FIG. 3.



P.A. Kraus et al.  
FIG. 4.



P.A. Kraus et al.  
FIG. 5.



P.A. Kraus et al.  
FIG. 6.